ELSEVIER

Sensors and Actuators B 73 (2001) 112–123

SENSORS AND ACTUATORS B CHEMICAL

www.elsevier.nl/locate/sensorb

Design, fabrication and vapor characterization of a microfabricated flexural plate resonator sensor and application to integrated sensor arrays

Brian Cunningham[a,*], Marc Weinberg[a], Jane Pepper[a,1], Chris Clapp[a], Rob Bousquet[a], Brenda Hugh[a], Richard Kant[b], Chris Daly[b], Eric Hauser[b]

[a]*Draper Laboratory, Woburn, MA 01801, USA*
[b]*Naval Research Laboratory, Woburn, MA 01801, USA*

Received 28 May 2000; received in revised form 12 September 2000; accepted 27 September 2000

Abstract

A chemical vapor detection and biosensor array based on microfabricated silicon resonators coated with thin film polymer sorption layers is described. The resonators within the array are micro-electromechanical (MEM) flexural plate wave (FPW) sensors that have been miniaturized to allow many independently addressable sensors to be integrated within a single silicon chip. The target analyte of an individual sensor within the chip is selected by placing a polymer coating onto the resonating membrane. Detection is performed by monitoring changes in the frequency and damping factor of the resonance as the coating interacts with the environment. This work documents vapor response characterization of an individual sensor element within an array and reports on the operation of an eight-element sensor array. Polymer coatings targeted toward detection of chemical weapon agents have been applied to the sensor and chemical vapor exposure tests using two chemical weapon simulants and four vapor phase interferents have been performed. Data describing temperature dependence, long-term/short-term drift stability, detection limits, detection linearity and vapor selectivity will be presented. The use of resonant damping information is shown to provide the ability to discriminate between vapor analytes that produce equal resonant frequency shifts.

Keywords: Gas sensors; Flexural plate waves; MEMS resonators; Sensor arrays

1. Introduction

Flexural plate wave (FPW) devices have demonstrated potential for a wide variety of chemical vapor and biochemical detection applications [1–4]. Through the application of a receptor coating to one side of the FPW resonating membrane, the interaction of the receptor with the environment is monitored by observing changes in the transducer's resonant frequency response. FPW devices have demonstrated the ability to function in vapor, liquid or aqueous gels, while the structure of the sensor permits it to have higher sensitivity at lower operating frequencies than bulk-wave or surface acoustic wave (SAW) devices of comparable dimensions [5–7].

In this work, the fabrication process and design of FPW sensors has been modified from previously reported structures to build a miniaturized FPW resonator. The miniaturized FPW resonator enables many identical FPW sensors to be integrated within a single chip without loss of detection sensitivity. Integrated arrays of FPW sensors will require spatially resolved application of receptor coatings, such as a microdroplet applicator, so that adjacent devices can be programmed to respond to different analytes. The ultimate goal of this work is the creation of a large multielement FPW array with several hundred devices operating within a single silicon chip. Micro-chemical analysis arrays (μCANARY) using miniature FPW sensors with appropriate molecular recognition chemistry will be capable of detecting vapor phase nerve agents, neuroactive peptide biochemical and infectious bacterial agents with much greater discrimination capability than single element systems. Further, because excitation and readout of the sensor elements is performed electronically at 10–20 MHz oscillator frequencies, the supporting hardware for the μCANARY will be small, rugged and inexpensive.

By making a large number of parallel sensor channels available, several system advantages are anticipated through the use of μCANARY sensors. First, the availability of multiple sensor redundancy is expected to reduce overall

* Corresponding author. Present address: SRU Biosystems, 10A Roessler Road, Woburn, MA 01801, USA.

[1] Present address: SRU Biosystems, 10A Roessler Road, Woburn, MA 01801, USA.

0925-4005/01/$ – see front matter
PII: S0925-4005(00)00664-X

measurement noise and to reduce the likelihood of false positive detection. Second, the ability to analyze a vapor sample's interaction with many receptor coatings is expected to improve the ability of vapor classification algorithms to perform accurate vapor identification. Third, the ability to incorporate FPW reference oscillators with close physical proximity and identical structure to 'live' sensor oscillators is expected to provide accurate compensation of common mode noise sources such as temperature variation, humidity variation and fluid flow variation.

Because the miniature silicon membrane resonators used in the μCANARY have not previously been tested for use as chemical vapor sensors, extensive characterization of their performance is necessary to demonstrate their utility and to verify analytical models that predict their performance. The purpose of this paper is to report on the characterization of individual sensor elements that will be used in a large sensor array. We have applied polymer thin films to the μCANARY that are often used to detect Sarin and Mustard chemical weapon agents [8,9]. Characterization was performed to measure sensor response to several types of challenges. The temperature dependence, long-term/short-term drift stability, detection limits, detection linearity and vapor selectivity have been characterized using exposure to chemical weapon simulants and four vapor phase interferents. The ability to utilize resonant damping shift information in addition to resonant frequency shift information to perform vapor discrimination is demonstrated for a single sensor. The application of this sensor technology to the detection of proteins in aqueous solution and to the detection and identification of bacteria and spores will be reported separately.

With the completion of individual sensor characterization, small format (eight-element) arrays were fabricated to demonstrate sensor uniformity and the ability to individually address specified sensor elements without crosstalk. The eight-element sensor array and electronics architecture is the platform that will be used to design integrated arrays of much larger size. In this report, we describe the first operating eight-element array in which individual elements can be selected electronically.

2. Experimental

2.1. Sensor design and fabrication

The fabrication sequence for building the Draper FPW resonator (cross-section diagram of a completed device is shown in Fig. 1A) begins with a purchased silicon-on-insulator (SOI) wafer (BCO Technologies, Belfast, UK). The SOI wafer upper surface is a 2 μm thick layer of epitaxial silicon bonded to a 1 μm thick layer of SiO_2. The SOI substrate is ~380 μm thick. A ~0.5 μm layer of piezoelectric AlN is deposited over the upper epitaxial silicon [10,11].

Vias for grounding contacts to the epitaxial silicon are provided by etching an opening into the AlN. Next, TiPtAu metalization of 0.1 μm total thickness is patterned to define interdigital metal electrodes, wire bond pad areas and ground contacts. Finally, the membrane is defined by etching a vertical sidewall cavity from the back side of the wafer with an inductively coupled plasma (ICP) etch machine using the Bosch process [12]. The 1 μm SiO_2 layer of the SOI substrate acts as an automatic etch stop for the ICP process. After the ICP etch is completed, the SiO_2 layer is removed by dipping the wafer into buffered hydrofluoric acid.

The layer thickness and metal electrode widths are selected to excite a membrane resonant mode of ~25 MHz in air. The electrodes are positioned within the membrane to align with eigenmodes of the resonating plate in order to maximize the amplitude of a particular resonant mode. The detailed modeling and design of the miniature FPW resonator are described in a separate publication [13]. SEM photos of a single miniature FPW sensor and several sensors within an array are shown in Fig. 1B and C. As shown in Fig. 1B, two sets of metal electrodes are utilized: one pair of electrodes applies a drive signal to excite the resonance, while the second set of electrodes senses the output response. The drive and sense electrode structures are identical and can be used interchangeably.

The electronics for the sensor are designed for open-loop operation through an interface with a network analyzer. The electronics require a source input from the analyzer and provide a reference signal (identical to sensor excitation) as well as the final gained output signal to the analyzer. The drive section consists of a high-gain single-ended input to differential output amplifier which is capable of driving capacitive loads at high frequency. The drive select uses a data select circuit to enable unique pairs of active FET switches allowing for individual differential drive of each sensor in the array. The pre-amp uses high-gain amplifiers configured as an instrumentation amplifier. This configuration allows for symmetrical loading on the sensor output, high common-mode signal rejection and higher gains for a given limited bandwidth.

2.2. Coating application

A poly methyl(4,4-bis(trifluoromethyl)-1-buten-4-01) siloxane polymer film was applied to the surface of the resonators in order to sensitize them to chemical weapon vapors [6]. The film, hereafter refered to as SXFA, was dissolved in chloroform and applied to the packaged sensor chip with an air brush. Because this application is performed manually, the amount of material deposited onto the sensor is monitored and controlled by simultaneously depositing polymer onto a reference quartz oscillator. The target coating thickness was 50 nm with a tolerance of 5 nm. After application of the coating, the polymer film is cured to evaporate solvent that is incorporated during the spraying process. A 60°C cure in an N_2 atmosphere for 3 days was sufficient to stabilize the film against any future mass change due to

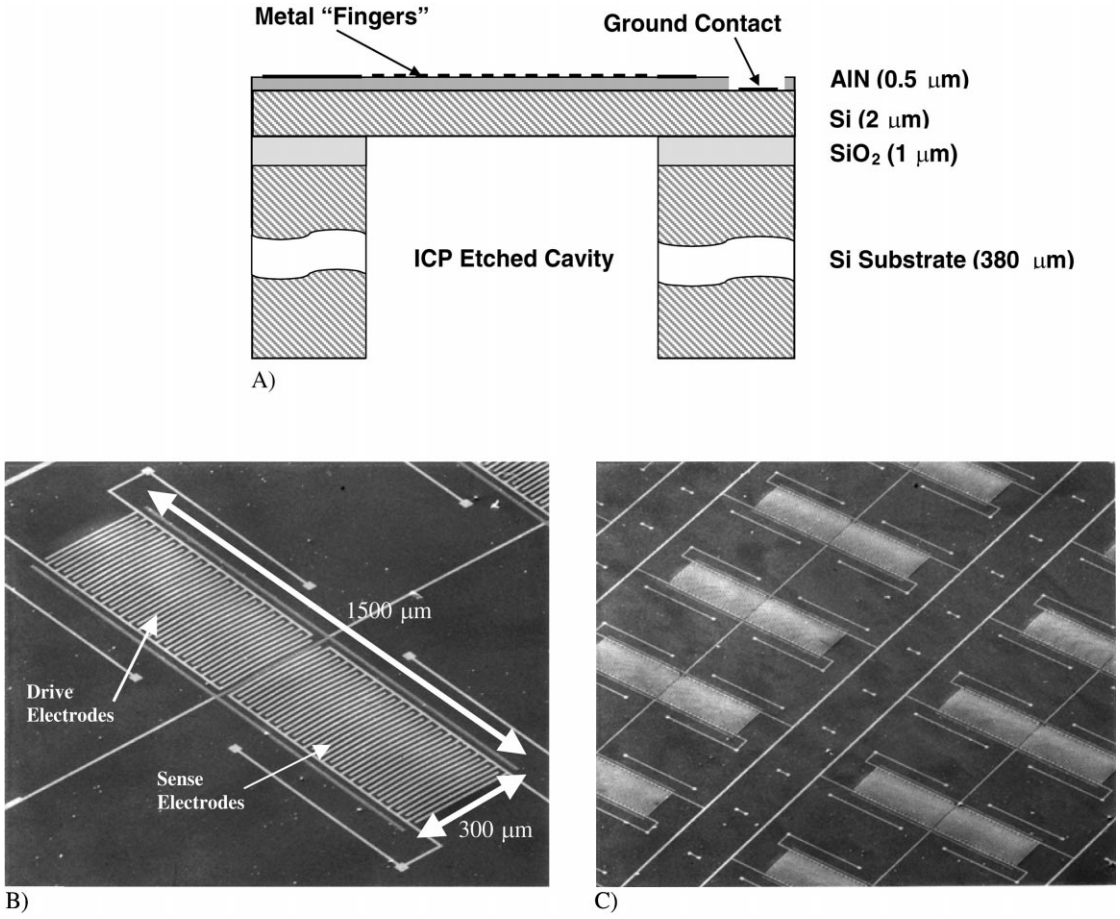

Fig. 1. (A) Cross-section diagram of the FPW resonating membrane structure; (B) SEM photo of a sensor element from the top surface of the wafer showing detail of metal electrode structure and (C) SEM photo of several integrated FPW membranes within a section of an integrated sensor array.

solvent loss. After the polymer coating is applied and cured, the sensor is loaded into the environmental exposure chamber and measured at constant temperature under flowing N_2 atmosphere to verify that that the coating has stabilized.

2.3. Sensor monitoring

A feature of all ultrasonic resonator chemical sensors is the ability of the sensor's resonant response to register changes in the viscoelastic properties of the polymer film as it absorbs vapor in addition to changes in the polymer film's mass [14–17]. For this reason, all the characterization tests measure both the sensor resonant frequency f_0 and the damping factor D of the resonance. The damping factor describes the width of the resonant mode in frequency space and is a dimensionless quantity defined as $D = f_0/\Delta f$ where Δf is the peak width at half-maximum. It will be shown that a single sensor has the ability to discriminate between many analytes based upon how the analytes affect D-even if each analyte produces an equal change in resonant frequency. The f_0 and D values are determined mathematically by measuring the FPW output signal as a function of frequency input and fitting the frequency response curve with a second order equation. The magnitude and phase response of a resonator is shown in Fig. 2. Resonant modes adjacent to the desired mode are typically observed at lower magnitude. Only the peak frequency and damping of the highest magnitude peak are tracked for the work reported. Typical devices fabricated with AlN piezoelectric thin film actuation register a peak signal 15–20 dB above background noise.

The time required per scan is 3.5 s, limited by the IEE 488 bus used to feed data from the readout instrument to the computer. The scan was limited to frequencies such that the response was greater than 70% of the peak response. This was done to reduce interference from nearby response peaks. The measurement algorithm consists of fitting the measured response to a fourth order expansion the inverse square of the admittance of a resonant device. Responses to five uniformly spaced frequencies nearly centered on the peak are fit to up to fourth order. Both the frequency at the response peak and the damping are determined from this fit.

2.4. Testing protocol

The test procedure is arranged to perform challenges to the sensor with increasing complexity. First, 'bare' sensors are tested without a polymer coating in order to later separate effects that are induced by the coating. Next, the

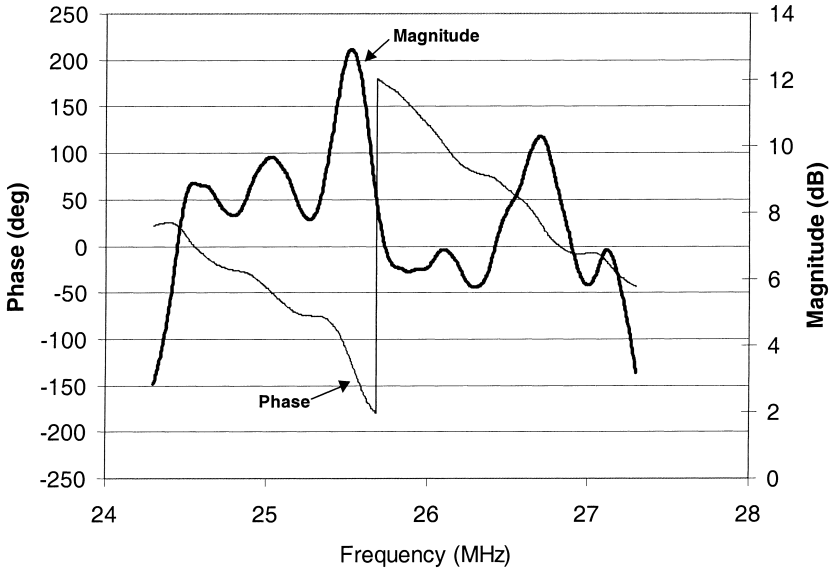

Fig. 2. Magnitude and phase spectra as a function of frequency for a typical μCANARY resonator fabricated with AlN piezoelectric thin film. The highest amplitude mode is identified and tracked to perform detection experiments.

coating is applied to the sensor and the response is monitored over an extended time period to assure the polymer is properly stabilized. When the coating is ready, variable temperature exposure tests are conducted using a fixed exposure concentration. Finally, for each analyte, variable concentration exposure tests are performed at fixed sensor temperature. Variable analyte concentration is used to determine response time, long-term memory effects, and ultimate detection limits.

The environmental chamber has a volume of 232 cm^3 and is made of nickel coated copper. It has a large thermal mass in order to maintain a uniform temperature throughout the sample volume. The chamber was equipped with a thermoelectric heater/cooler that is part of a computer driven, closed loop, temperature controller that holds the chamber temperature to within 0.01 K of the set point. The vapor source is a microsensor systems vapor generator set to deliver analytes in nitrogen gas at a flow rate of 100 sccm with analyte concentrations ranging from 0.00063 of saturation to 0.125 of saturation. Neglecting sorption effects, the time constant for changing the sample concentration in the chamber was estimated to be 3 min. The effects of temperature changes on the analyte concentration were minimized by constrictions in the flow path. In this constant volume approximation, a increase in temperature produces an increase in pressure rather than a decrease in concentration. For all analytes (except dimethyl-methyl phosphonate (DMMP)), the peak concentration was 1/8 of saturation. For DMMP it was 1/16 of saturation. In all cases, the smallest non zero concentration was 1/100 of the corresponding peak value. During concentration ramping the concentration change in increments of 1/100 of the corresponding peak value.

To establish a baseline against which all exposure tests can be compared, the sensor is first exposed to a constant flow of dry N_2 and the f_0 and D are measured over a temperature range of 10–75°C. For temperature-dependence testing, the sensor response is measured while the temperature is ramped up and ramped down in order to identify the presence of hysteresis. The N_2-exposed temperature data for the coated sensor is subtracted from the N_2-exposed temperature data for the uncoated sensor to determine the temperature dependence of the coating. The temperature response of f_0 and D are shown in Fig. 3. Next, the coated sensor is held at constant temperature and N_2 flow for an extended time period to quantify short-term noise and drift.

With the N_2-exposed response fully characterized, analyte vapors are introduced into the sample stream one at a time. The total flow rate is held constant and the vapor concentration of each analyte is held constant while the temperature is ramped between 10–75°C (both upward and downward). The vapor is obtained by bubbling N_2 through a glass vial containing the analyte in liquid form. All the analyte vials are held at a constant temperature of 15°C and the sensor exposure concentration is controlled by mixing additional N_2 with the output of the bubbler. The exposure concentration for each vapor is selected to be less than 10% of the vapor saturation value of N_2 at 15°C. The analytes studied were methanol, toluene, octane, chloroform, DMMP nerve agent simulant and chloro-ethyl ether (CEE) mustard agent simulant.

The rate at which the sensor responds to a step function exposure to an analyte was measured. The test is performed by setting the sensor temperature to a fixed value, passing a fixed gas flow rate into the exposure chamber and alternately turning on and turning off the flow of analyte vapor. A 3 h 'off' period is followed by a 3 h 'on' period and the on/off cycle is repeated three times. The long time period is used to measure the long-term time constant of the interaction between the coating and the analyte, and to measure the

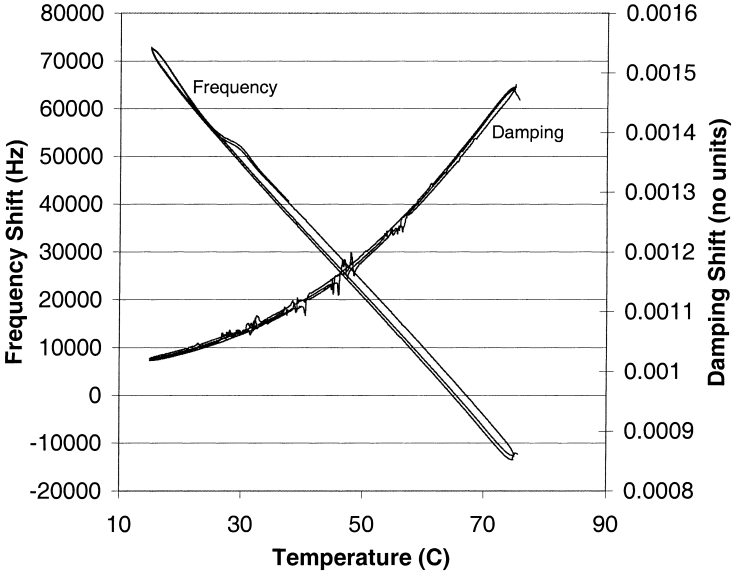

Fig. 3. Temperature dependence of resonant frequency and damping.

extent to which a coating retains memory of past exposures. The test is performed with a single analyte exposed to the sensor at a time and the test is repeated for each of the analyte vapors.

The final characterization test is to measure the sensor response as a function of analyte concentration to determine response linearity and sensitivity limits. The sensor temperature and total gas flow rate are held constant while the concentration of a single analyte is slowly ramped up to a maximum value, and then ramped down to zero. While this test provides data on frequency shift and loss shift as a function of analyte concentration, ($f_0([C])$ and $D([C])$), we may also use the data generated by this experiment to determine the relationship between frequency shift and loss shift $f_0(D)$ for the analytes. It has been shown that absorbed analytes which produce identical changes in f_0 shift may be discriminated by differentiated changes in D. This experiment will be used to quantify the relationship between f_0 shift and D shift and to determine the concentration limits in which the technique has discrimination value.

3. Results

3.1. Short-term drift

Fig. 4 shows a measurement of f_0 and D over a 40 min time period. The measurement shows that the resonant frequency measurement can vary within a ~8 Hz window. The error window determined by this measurement directly

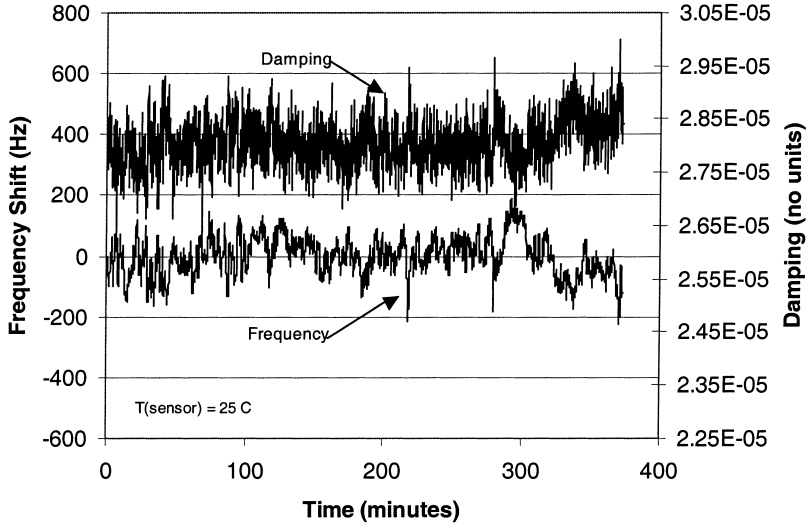

Fig. 4. Frequency as a function of time for a μCANARY resonator.

affects the lower order detection limit of the sensor. The uncertainty of frequency and damping quantification is, in turn, directly correlated to the D of the sensor resonance. Damping of $0.00125 < D < 0.002$ are typically obtained for currently fabricated structures.

3.2. Exposure testing

3.2.1. Frequency and damping shift over temperature

Fig. 5 shows the resonant frequency and damping shift as a function of temperature for the SXFA-coated μCANARY individually exposed to the vapor analytes. The largest signals are obtained at the lowest temperature, as lower temperature conditions favor sorption of analyte within the polymer film. Because the exposure concentration of each analyte is different, the data in Fig. 5 must be normalized (frequency shift or damping shift divided by exposure concentration) to observe the actual vapor selectivity afforded by the coating. The normalized data, shown in Fig. 6, shows that the largest responses are obtained for DMMP and to a lesser extent, CEE. Fig. 6 shows that the SXFA–coating is extremely effective at detecting DMMP

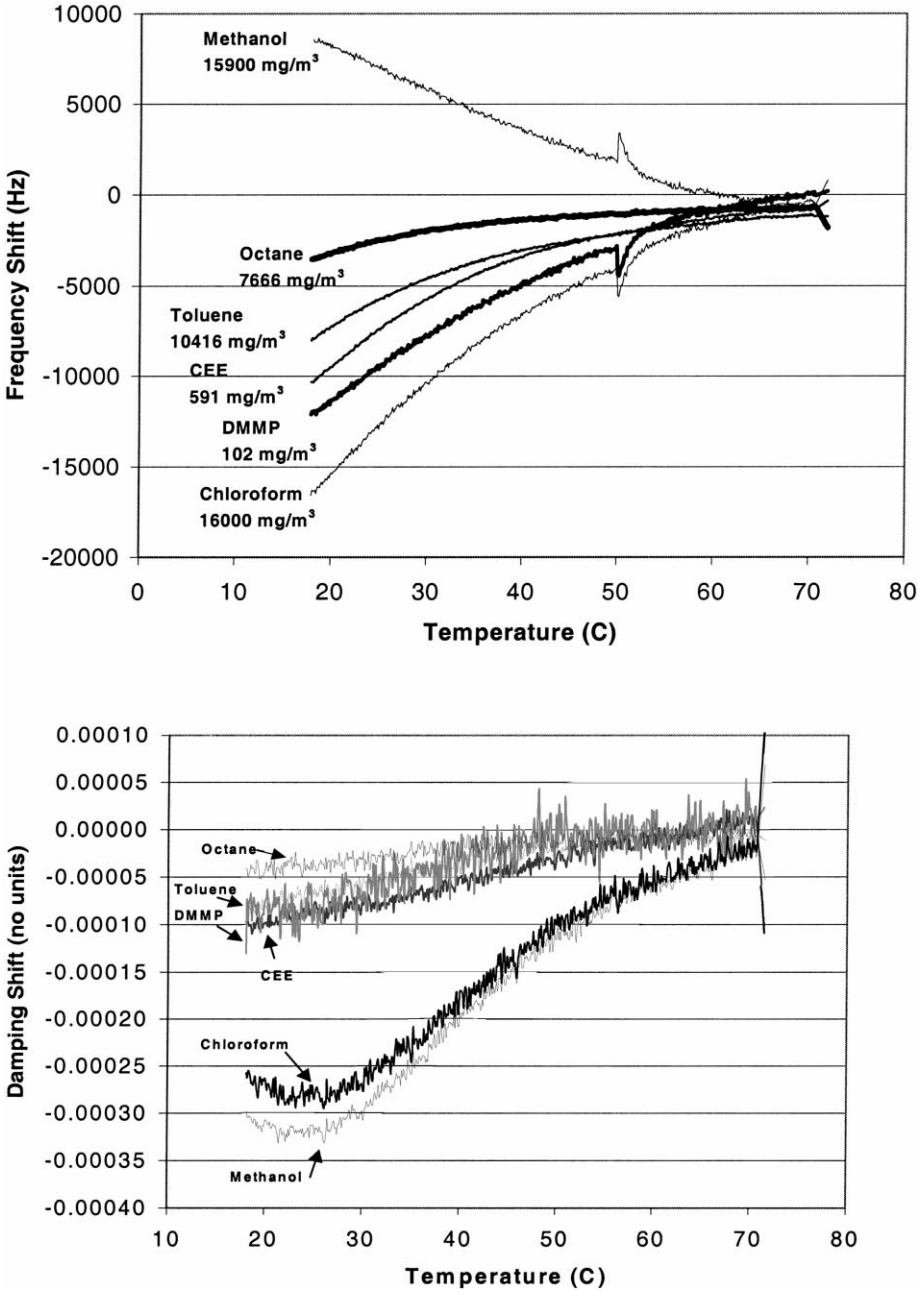

Fig. 5. Frequency and damping shift as a function of temperature for SXFA-coated μCANARY sensor exposed individually to six vapor analytes of various concentrations.

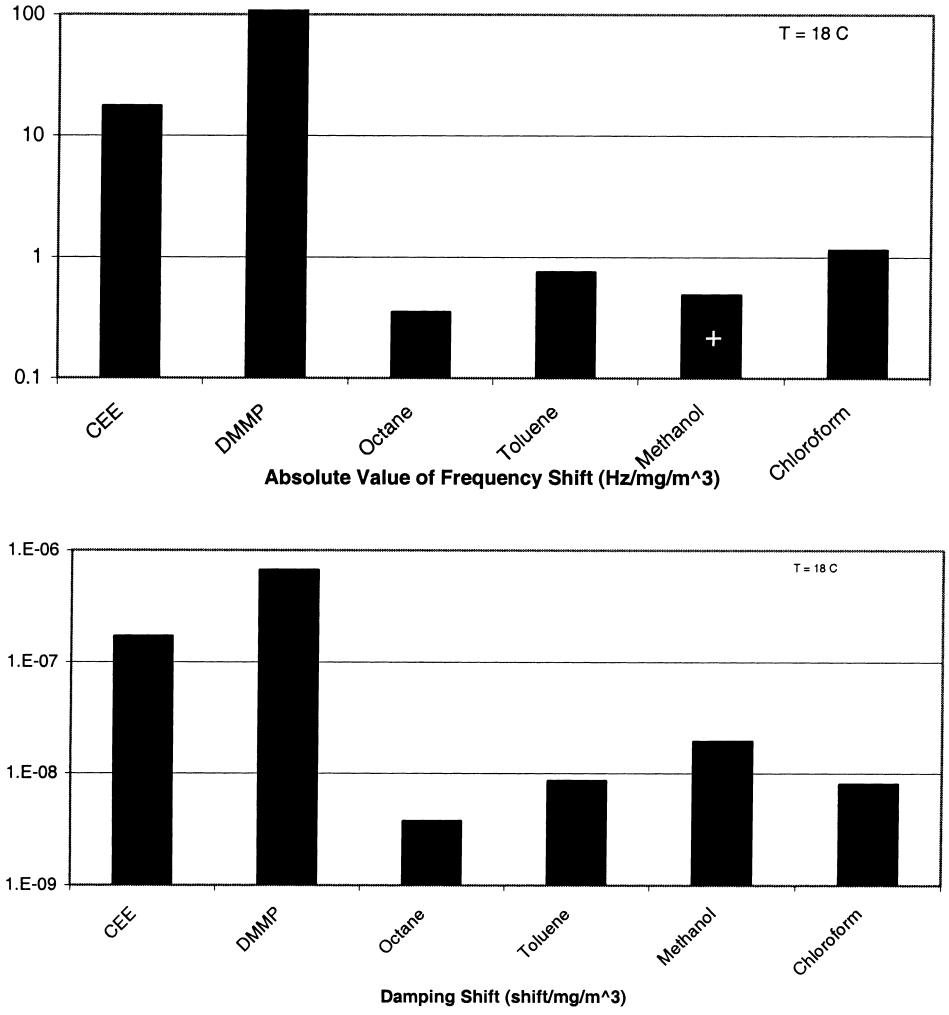

Fig. 6. Normalized frequency and damping shift of a SXFA-coated μCANARY sensor to several vapor analytes.

compared to toluene (156:1 Δf selectivity), methanol (243:1 Δf selectivity) and octane (334:1 Δf selectivity). While most analytes generate a negative frequency shift when sorbed into the polymer coating, methanol was repeatedly observed to induce a positive frequency shift. The cause of the positive frequency shift is assumed to be due to generation of stress in the polymer film that results in application of tension on the resonating membrane. This counterintuitive result highlights

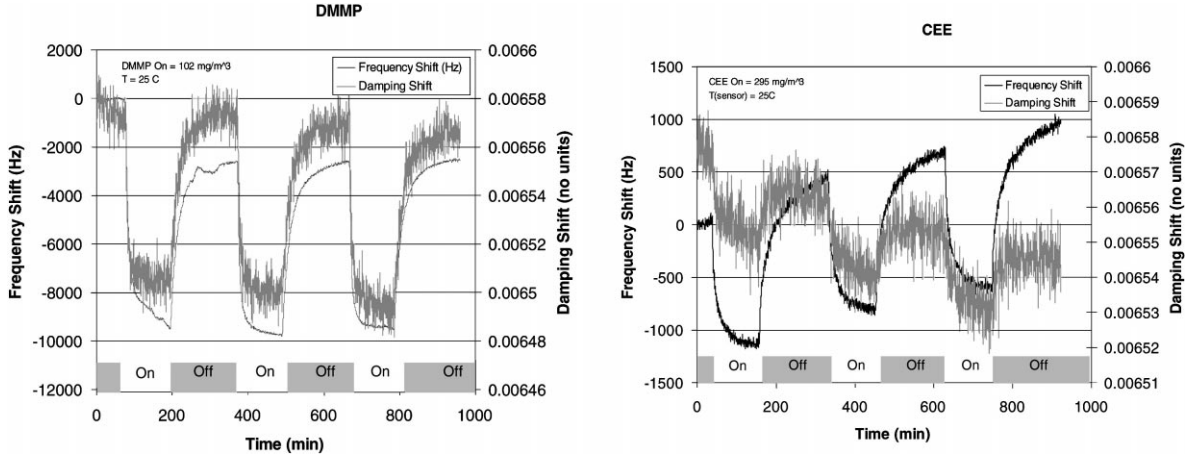

Fig. 7. Frequency and damping shift response to on/off exposure testing of two representative vapor analytes. The sensor response time is limited by the dead volume and internal surface sorption of the exposure chamber, so observed switching times are not indicative of the intrinsic sensor response rate.

the fact that acoustic wave sensors respond to mass adsorption as well as to changes in the mechanical properties of the polymer coating.

3.2.2. On/off exposure tests

The frequency shift and damping shift response of an SXFA-coated μCANARY to the on/off exposure sequence to two of the six analytes are shown in Fig. 7. The observed time constants for sensor response and differences noted between analytes are the result of the time required to fill the exposure chamber with an equilibrium concentration of analyte vapor at low concentration. Vapor molecule sorption and desorption to the internal surfaces of the exposure chamber and gas introduction lines results in a response latency that is dependent upon the affinity of each particular vapor for the internal surfaces of the environmental

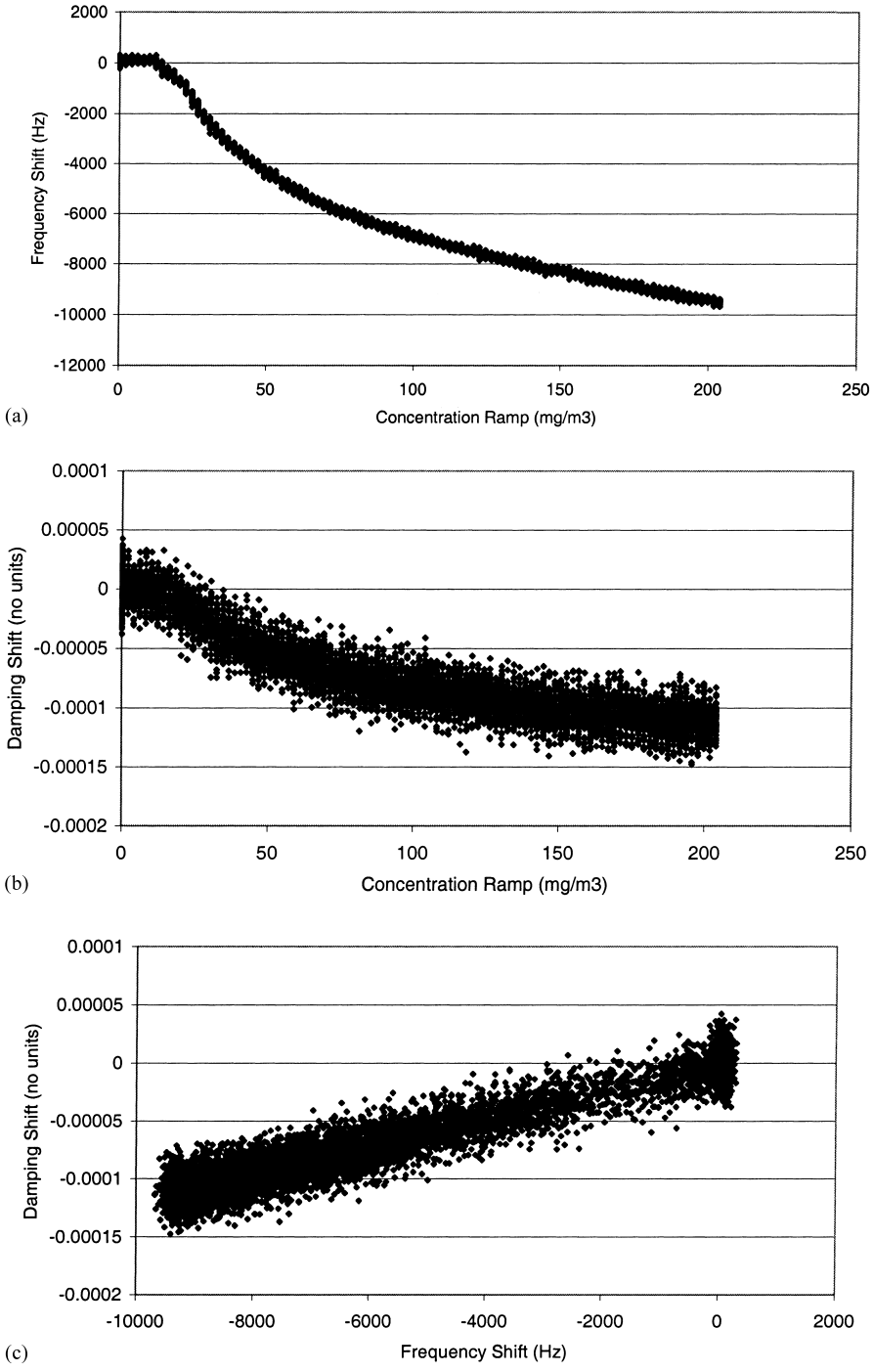

Fig. 8. Frequency shift and damping shift as a function of vapor concentration for SXFA-coated μCANARY exposed to DMMP and the linear relationship between frequency and damping shift that is characteristic of this particular analyte.

chamber, and do not therefore represent the response time constant of the sensor.

3.2.3. Concentration-ramped exposure tests

The frequency and damping shift as a function of analyte concentration for an SXFA-coated μCANARY exposed to DMMP at a ramp-up rate of 2 mg/m^3/min is shown in Fig. 8a and b. Although, the sensor response was measured while the concentration was ramped up and ramped down, only data for the ramp-up portion of the test are shown in Fig. 8 for clarity. By combining the data in Fig. 8a and b, the relationship between frequency and damping shift can be obtained and is shown for DMMP in Fig. 8c. A linear *f/D* relationship is observed for the SXFA-coated sensor exposed to DMMP. The frequency and damping shift as a function of concentration was measured for each of the six vapor analytes (data not shown) and linear *f/D* relationships were observed for each vapor. As we will show, the *f/D* relationship can be used as a tool to discriminate between vapor analytes that produce identical frequency shift responses.

4. Discussion

4.1. Vapor discrimination based on frequency and damping shift

A basic problem underlying all vapor sensors that utilize a polymer coating to sorb analyte vapor is that no coating displays complete selectivity to every possible interferent. While chemical weapon vapors must be detected at levels less than 100 ppb, benign substances such as methanol and octane are likely to be encountered at 100 ppm levels. Therefore, even receptor coatings with 1000:1 selectivity can yield false responses or miss detection of a target analyte in the presence of high concentrations of interferent. Because a sensor operating outside the laboratory is likely to encounter combinations of unknown analytes of unknown concentrations, a number of approaches are being developed to reduce the false negative/false alarm rate of chemical weapon detection systems to acceptable levels. One method is to rely on the use of multiple sensors with multiple coatings that can provide a response 'signature' that can be interpreted by a neural network computer algorithm [18]. A second method is to combine a coating-based sensor with a 'front-end' vapor separation device such as a gas chromatography (GC) or field-assisted ion mobility (FAIM) spectrometer, that can reduce the identification computation complexity by assuring that the sensor coating is only exposed to one analyte at a time [19].

In either case, the ability to extract the maximum amount of information from an exposed sensor is a key for performing accurate vapor identification with a minimum false negative/false alarm rate. As shown in this work, the μCANARY sensor responds to sorption of vapor in two distinct ways. First, sorption of mass on the sensor membrane results in a frequency shift caused by an increase in the mass density of the membrane structure. Secondly, the sorbed analyte changes the mechanical properties of the

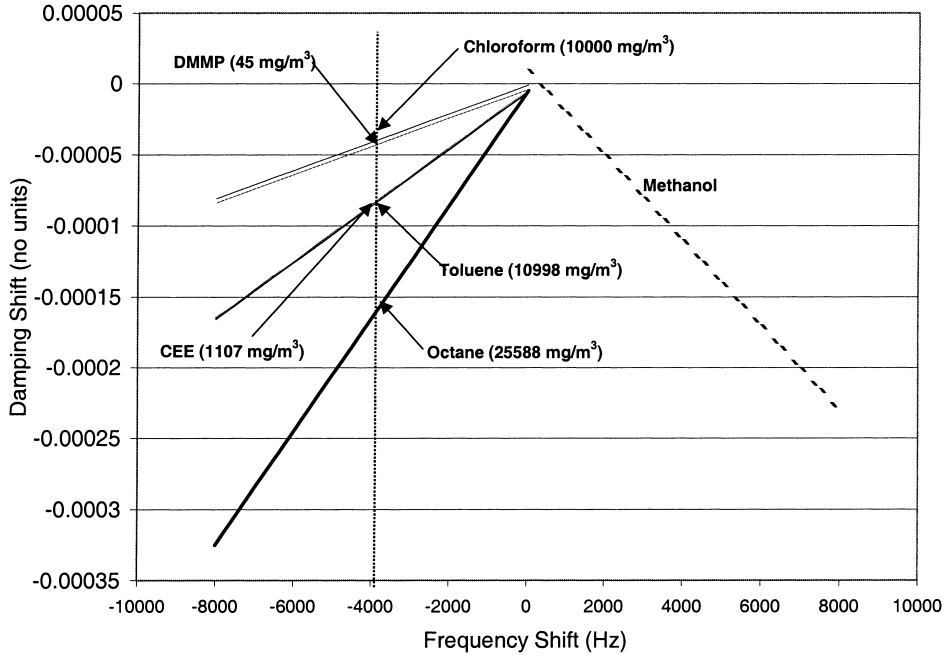

Fig. 9. Frequency change as a function of damping change for an SXFA-coated μCANARY exposed to the six vapor analytes. The *f* vs. *D* relationships shown represent straight-line fits to the actual data as in Fig. 8c for DMMP and do not convey the noise present.

polymer receptor film and the mechanical changes can be monitored by measuring the damping of the membrane resonance. The damping responses and the frequency shift responses are characteristic for the vapor/coating combination. They are repeatable and related in a predictable, easily modeled way.

Fig. 8c shows how the resonant frequency of the sensor and the damping are related to the concentration of a single vapor analyte, DMMP. When the *f*/*D* relationship for each of the vapors to the coated sensor are plotted together, as shown in Fig. 9, one can see how the damping response can be used as a tool for vapor identification. If one assumes that only one vapor analyte is exposed to a single sensor, Fig. 9 shows that it is possible for several vapors to produce a 4000 Hz frequency shift on the sensor. For example, because the selectivity of the SXFA-coating is not perfect, a 45 mg/m^3 exposure of DMMP produces an identical frequency shift as a 11 000 mg/m^3 exposure of toluene. However, only DMMP and chloroform have the ability to induce a 4000 Hz frequency shift and a damping shift of -0.0005. Therefore, using a single sensor, the field of possible unknown analyte vapors can be narrowed significantly. A second sensor with a different polymer coating that provides a differential *f*/*D* relationship between DMMP and chloroform would be required to perform unique discrimination. Once discrimination is obtained, any of the *f*/*D* relationships can be used to determine the analyte concentration.

4.2. Detection limits

The detection sensitivity limit of the polymer coated μCANARY sensor to CW agent is determined by the analyte exposure concentration that produces a minimum statistically significant signal. The minimum detectable frequency shift is determined by the frequency stability of the detector and electronics. While closed-loop oscillator instrumentation has enabled a frequency standard deviation (S.D.) of 2.5 Hz, the open-loop instrumentation used for the vapor exposure tests reported here have a typical rms scatter of 80 Hz for sensors with $D = 0.002$. Typically, a signal that is three times larger than the standard deviation is considered to be a statistically significant signal that a detection algorithm would identify as a meaningful event. Therefore, the minimum observable frequency shift for detection is 240 Hz.

The minimum concentration of DMMP that is detectable by the sensor is that which produces a 240 Hz frequency shift. For DMMP exposure, it was shown in Figs. 7 and 8 that the SXFA-coated μCANARY produces a frequency shift of -100 Hz for every mg/m^3 of DMMP. Therefore, the minimum detectable concentration of DMMP is 2.4 mg/m^3. Using closed-loop oscillator instrumentation should enable sensitivity of 0.075 mg/m^3 to be obtained.

Although, we have achieved a precision of 10 ppm in measured values of $D = 1/Q$ for other systems, the best we have done with the FPW device is 1000 ppm. In addition, the precision in the determination of the frequency at the peak is much greater than that for *D*, at about 3 ppm. This precision is also about second orders of magnitude less than achieved in work on other resonant systems. Although, the differences in precision for the frequency and damping measurements is offset somewhat by a relatively large damping response, the damping response can be used to discriminate between analytes only for the larger concentrations. It is important to note, however, that the polymer film used in these experiments was in no way optimized to enhance the analyte-induced damping response. We speculate that it will be possible to significantly increase the damping response by tailoring the structure of the coating. The laboratory instrument used for the reported tests is designed for precision and accuracy, but not for speed. In general, the precision of the measurement increases with integration time since the time average value of statistically uncorrelated quantities (such as noise) decreases as the square root of the measurement time.

4.3. Eight-element μCANARY

For a sensor array with multiple elements, a single 'drive' circuit is addressed through a multiplexer to excite only one element within the array at a time. A single 'sense' circuit is connected to all devices within the array in parallel. Using this circuit configuration the number of electronic components required to operate the array is minimized. Linear array chips with eight sensor elements were fabricated and packaged to interface with the addressable electronic readout. The sensor address was sequentially selected to address individual sensors within the array. The magnitude and phase output of the sensors were stored and the resulting magnitude traces are shown in Fig. 10. Each of the sensors within the array was functional. Fig. 10 shows that the sensors within the array are not absolutely identical, and that each device has a slightly different resonant frequency so that each sensor can be uniquely identified. While the frequency of maximum output varied across the array, the resonant frequency phase was within a 5° range. This amount of phase variation will allow a single excitation and output amplification circuit to resonate all the devices within the array without including automatic phase-adjusting components. This ability significantly reduces the complexity of the μCANARY electronics. At this time, we believe that closed-loop oscillatory operation of sensors should be used to quickly and accurately obtain resonant frequency information, and that an open-loop scan centered around the resonant peak should be used to determine the resonant damping. Measurements are currently taken by scanning frequencies surrounding the resonant peak and mathematically determining *D*. Measurement duty cycle is limited to several seconds per sensor by the interface between a spectrum analyzer instrument and a computer that controls the peak scanning protocol. The Draper Laboratory group is currently developing an electronic interface to the

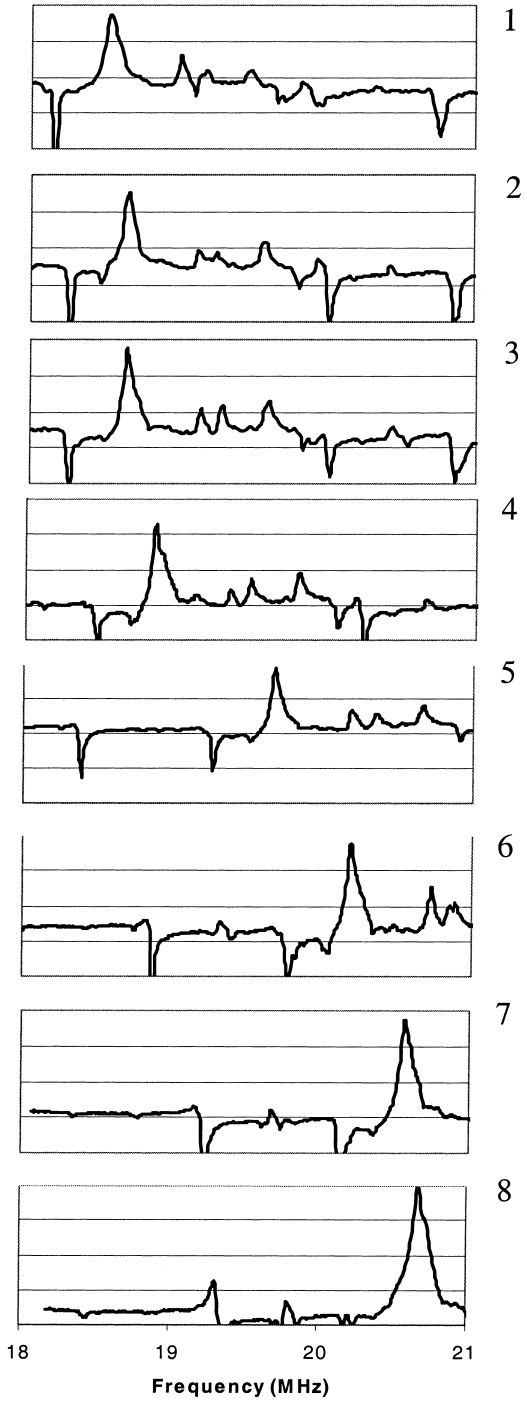

Fig. 10. Frequency response of eight individual μCANARY elements within an array chip sequentially selected by addressing electronics.

sensor to reduce the duty cycle of a sensor measurement to less than 0.1 s per sensor.

5. Conclusion

In this work, a new fabrication process for building miniature FPW sensors for integrated arrays has been demonstrated. Thorough characterization of individual sensors has been carried out through the application of a thin polymer film and a series of vapor exposure tests under controlled laboratory conditions. Both resonant frequency changes and resonant damping changes were monitored in response to changes in temperature, vapor analyte, and analyte concentration. Like other acoustic resonator sensors, changes in the viscoelastic properties of the polymer coating are registered as both changes in resonant frequency and resonant damping coefficient. The resonant damping information can be used to provide additional discrimination information to identify vapors that have differing *f*/*D* relationships, provided that exposure concentration is high enough to overcome noise in the f and D measurements themselves. As expected, the sensitivity of the miniature FPW sensors is similar to that reported for larger FPW membranes, which is typically determined by the resonator membrane mass/area.

The first eight-element integrated array of FPW sensors using the new fabrication approach has been demonstrated, which will allow simultaneous detection of multiple chemical interactions through the selective application of different coatings onto individual sensors using a microdroplet applicator. Future work will involve developing methods for application of coatings to individual sensors and vapor exposure testing of the array. Future work will target building large format array structures along with their associated packaging, electronics and software. Finally, the use of the μCANARY sensor array for the unlabelled gravimetric detection of biologically relevant materials, such as proteins, peptides and intact microorganisms is currently under investigation.

Acknowledgements

The authors wish to thank DARPA and Program Manager Ed Gjermundsen (Contract N00174-97-D-0030) for providing the funding that was used to perform the work at Draper Laboratory. We are indebted to Dr. R. Andrew McGill at NRL for suggesting and providing the polymer coating used in these experiments. B. Cunningham acknowledges the valuable technical discussions and MEMS fabrication advice provided by Jon Bernstein and Jeff Borenstein. Connie Cardoso and the staff within the Draper MEMS fabrication facility are acknowledged for their valuable assistance in device fabrication. AlN piezoelectric thin films were provided through the Massachusetts Institute of Technology by Prof. Rafael Reif and Draper Fellow students Peter Hsieh and Wendy Mao. The characterization tests were performed jointly between Draper Laboratory and NRL. Draper Laboratory provided packaged sensors and sensor excitation/readout electronics to NRL for exposure test experiments. All subsequent polymer deposition and qualification tests were performed at NRL. Thanks to T.J. Boberek for assistance with preparation of the figures.

References

[1] S.W. Wenzel, R.M. White, Flexural plate-wave gravimetric chemical sensor, Sens. Actuat. A A21–A23 (1990) 700–703.

[2] J.W. Grate, S.W. Wenzel, R.M. White, Flexural plate wave devices for chemical analysis, Anal. Chem. 63 (1991) 1552–1561.

[3] R.M. White, S.W. Wenzel, US Patent 5,129,262, Plate-Mode Ultrasonic Sensor, July, 1992.

[4] Q.-Y. Cai, J. Park, D. Heldsinger, M.-D. Hsieh, E.T. Zellers, Vapor recognition with an integrated array of polymer coated flexural plate wave sensors, Sens. Actuat. B 62 (2000) 121–130.

[5] S.W. Wenzel, R.M. White, Analytical comparison of the sensitivities of bulk-wave, surface-wave and flexural plate-wave ultrasonic gravimetric sensors, Appl. Phys. Lett. 54 (20) (1989) 1976.

[6] G.W. Watson, W. Horton, E.J. Staples, GAS chromoatography utilizing SAW sensors, in: Proceedings of the Ultrasonics Symposium, 1991, pp. 305–309.

[7] T. Hofmann, P. Schieberle, C. Krummel, A. Freiling, J. Bock, L. Heiert, D. Kohl, High resolution gas chromatography/selective odorant measurement by multisensor array (HRGC/SOMSA): a useful approach to standardize multisensor arrays for use in the detection of key food odorants, Sens. Actuat. B 41 (1997) 81–87.

[8] J.W. Grate, A. Snow, D.S. Ballantine Jr., H. Wohltjen, M. Abraham, R.A. McGill, P. Sasson, Determination of partition coefficients from surface acoustic wave vapor sensor responses and correlation with gas–liquid chromatographic partition coefficients, Anal. Chem. 60 (1988) 869.

[9] R. Andrew McGill, M.H. Abraham, J.W. Grate, Choosing polymer coatings for chemical sensors, Chemtech, 1994, p. 27.

[10] P. Hsieh, R. Reif, B. Cunningham, DC magnetron reactive sputtering of low stress aluminum nitride piezoelectric thin films for MEMS applications, in: Proceedings of the Material Research Society Fall Meeting, 1998, Boston, MA.

[11] R.P. O'Toole, S.G. Burns, G.J. Bastiaans, Thin aluminum nitride film resonators: miniaturized high sensitivity mass sensors, Anal. Chem. 64 (1992) 1289–1294.

[12] F. Laermer, A. Schilp, Method of anisotropically etching silicon, US Patent 5,501,893.

[13] M. Weinberg, B. Cunningham, C. Clapp, Modeling of flexural plate wave resonators, JMEMS, in press.

[14] R.A. Kant, C.L. Daly, H.-D. Wu, Chemical Identification Using Internal Friction and Frequency Measurements on a Polymer Coated Resonator, EFTF-IEEE IFSC, Besancon, France, 13–16 April, 1999.

[15] A.J. Ricco, S.J. Martin, Multiple-frequency SAW devices for chemical sensing and materials characterization, Sens. Actuat. B 10 (1993) 123–131.

[16] G.C. Frye-Mason, S.J. Martin, Sens. Mater. 2 (1991) 187–195.

[17] S.J. Martin, A.J. Ricco, in: Proceedings of the IEEE Ultrasonics Symposium, Montreal, 1989, p. 621–625.

[18] E.T. Zellers, S.A. Batterman, M. Han, S.J. Patrash, Optimal coating selection for the analysis of organic vapor mixtures with polymer coated surface acoustic wave sensor arrays, Anal. Chem. 67 (1995) 1092.

[19] G.C. Frye-Mason, R.J. Kottenstette, P.R. Lewis, R.P. Manginell, S.A. Casalnuovo, E.J. Heller, C.M. Matzke, W.K. Schubert, V.M. Hietala, M.L. Hudson, C.C. Wong, C.J. Brinker, D.Y. Sasaki, J.W. Grate, Miniaturized chemical analysis systems for selective and sensitive gas phase detection, in: Proceedings of the 29th International Conference on Environmental Systems, in press.